


Cardiac Dose Control and Optimization Strategy for Left Breast Cancer Radiotherapy With Non-Uniform VMAT Technology

Technology in Cancer Research & Treatment
 Volume 20: 1-9
 © The Author(s) 2021
 Article reuse guidelines:
sagepub.com/journals-permissions
 DOI: 10.1177/15330338211053752
journals.sagepub.com/home/tct


Jianjian Qiu, PhD , Shujun Zhang, MS, Bo Lv, MS, and Xiangpeng Zheng, MD

Abstract

Purpose: A novel in-house technology “Non-Uniform VMAT (NU-VMAT)” was developed for automated cardiac dose reduction and treatment planning optimization in the left breast radiotherapy. **Methods:** The NU-VMAT model based on I_{GM} (gantry MLC Movement coefficient index) was established to optimize the volumetric modulated arc therapy (VMAT) MLC movement and modulation intensity in certain gantry angles. The ESAPI embedded in Eclipse® was employed to connect TPS and the optimization program via I/O relevant DICOM RT files. The adjuvant whole-breast radiotherapy of 14 patients with left breast cancer was replanned using our NU-VMAT technology in comparison with VMAT and IMRT technology. Dosimetric parameters including $D_{1\%}$, $D_{99\%}$, and D_{mean} of PTV, V_5 , V_{10} , and V_{20} of ipsilateral lung, V_5 , D_{20} , D_{30} , and D_{mean} of heart, monitor units (MUs), and delivery time derived from IMRT, VMAT, and NU-VMAT plans were evaluated for plan quality and delivery efficiency. The quality assurance (QA) was conducted using both point-dose and planar-dose measurements for all treatment plans. **Results:** The $I_{GM-NU-VMAT}$ curves with plan optimization (range from 50% to 147%) were converged more significantly than $I_{GM-VMAT}$ curves (range from 0% to 297%). The dose distribution requirements of the target and normal tissues could be met using IMRT, VMAT, or NU-VMAT; the lowest D_{mean} was achieved in NU-VMAT plans (5.38 ± 0.46 Gy vs 5.63 ± 0.61 Gy in IMRT and 7.95 ± 0.52 Gy in VMAT plans). Statistically significant differences were found in terms of delivery time and MU when comparing IMRT with VMAT and NU-VMAT plans ($P < .05$). In comparison with IMRT plans, the MU and delivery time in NU-VMAT plans dramatically decreased by 69.8% and 28.4%, respectively. Moreover, NU-VMAT plans showed a high gamma passing rate ($96.5\% \pm 1.11$) in plane dose verification and minimal dose difference ($2.4\% \pm 0.19$) in point absolute dose verification. **Conclusion:** Our non-uniform VMAT facilitated the treatment strategy optimization for left breast cancer radiotherapy with dosimetric advantage in cardiac dose reduction and delivery efficiency in comparison with the conventional VMAT and IMRT.

Keywords

breast cancer, cardiac dose, non-uniform volumetric modulated arc therapy (NU-VMAT), intensity-modulated radiation therapy, optimization

Abbreviations

AAA, anisotropic analytical algorithm; BEV, beam’s eye view; CBCT, cone-beam CT; CI, Conformity index; CRT, conformal radiotherapy; DVH, dose-volume histogram; ESAPI, Enterprise Security Application Programming Interface; GTV, gross tumor volume; IMRT, intensity-modulated radiation therapy; ITV, internal target volume; MLC, Multi-Leaf Collimator; MU, monitor unit; NU-VMAT, Non-Uniform Volumetric Modulated Arc Therapy; OAR, organ-at-risk; PTV, planning target volume; QA, quality assurance; RIHD, Radiation-induced heart disease; RT, Radiation Therapy; VMAT, Volumetric Modulated Arc Therapy

Received: February 26, 2021; Revised: September 22, 2021; Accepted: September 29, 2021.

Introduction

Breast cancer is one of the most common malignant tumors in women. The incidence of breast cancer is increasing year by year.¹ Radiotherapy has been playing an indispensable role in the management of breast cancer, and numerous clinical studies have shown that postoperative radiotherapy after breast-conserving

Huadong Hospital, Fudan University, Shanghai, China

Corresponding Author:

Xiangpeng Zheng, MD, Department of Radiation Oncology, Huadong Hospital, Fudan University, 221 West Yan’an Road, Shanghai 200040, China.
 Email: zhengxp@fudan.edu.cn



Creative Commons Non Commercial CC BY-NC: This article is distributed under the terms of the Creative Commons Attribution-NonCommercial 4.0 License (<https://creativecommons.org/licenses/by-nc/4.0/>) which permits non-commercial use, reproduction and distribution of the work without further permission provided the original work is attributed as specified on the SAGE and Open Access page (<https://us.sagepub.com/en-us/nam/open-access-at-sage>).

surgery (BCS) can reduce the recurrence rate and improve the survival rate of patients.² However, it has been reported that the ionizing radiation from left breast radiotherapy is associated with the increasing incidence of heart disorders, especially coronary disease. Radiation-induced heart disease (RIHD) has become one of the major concerns related to nonneoplastic death in patients receiving left breast radiotherapy.¹⁻⁵

Currently, three-dimensional conformal radiation therapy (3D CRT), intensity-modulated radiation therapy (IMRT), volumetric modulated arc therapy (VMAT), and Tomotherapy are commonly used in the treatment planning of breast cancer radiotherapy.⁶⁻¹⁴ Comparative studies have shown that benefiting from the reverse optimization strategy IMRT and VMAT can achieve better dose distribution to the target and less dose exposure to the adjacent organs at risk than CRT.¹² Since the left breast is located in the vicinity of the heart, which makes the heart unavoidable to the radiation during the left breast radiotherapy. Studies have shown that for each 1 Gy increase in the average cardiac dose, the incidence of radiation-induced coronary artery-related events increases linearly by 7.4% without the apparent threshold.⁵ Therefore, it is necessary to optimize the existing technologies or develop an advanced strategy to minimize the cardiac dose while maintaining the proper dose coverage in the target. Several techniques based on IMRT, VMAT, and tomotherapy have been developed with reported equivocal benefits in cardiac sparing.⁷⁻¹¹

Based on the conventional VMAT model, we developed a novel two-stage optimization method, “Non-Uniform VMAT (NU-VMAT),” by removing unnecessary beams to reduce dose to OARs while maintaining sufficient dose coverage to targets. In this study, the performance of NU-VMAT was evaluated in comparison with conventional IMRT in terms of plan quality and delivery efficiency.

Materials and Methods

Non-Uniform VMAT Mathematic Model

All the sub-fields in a 360° arc are distributed uniformly in the conventional VMAT mathematical model, suggesting that radiation dose would exist in all sub-fields around the patient (Figure 1a). Current VMAT may over-modulate in certain directions since some sub-fields are insignificant for target dose and only contribute to extra dose to normal structure and increase whole-body low-dose radiation. Thus, the concept of NU-VMAT (Non-Uniform Volumetric Modulated Arc Therapy) is proposed and established in this study by eliminating insignificant segments while increasing the radiation intensity of the remaining significant fields. Unlike VMAT, the gantry rotation speed can be changeable appropriately by the NU-VMAT algorithm. Two clinical scenarios were taken into consideration in the NU-VMAT model to improve the intensity modulation and treatment quality. At the circumstance of low-speed gantry rotation matching fast MLC motion, multiple sub-fields radiations can be completed by the rapid MLC movement, or the modulation intensity can be increased by extending partial arc (Figure 1b, arrow ①). On the contrary, when high-speed gantry rotation matches static MLC, large-field radiation can be completed while creating multiple beam-off fields simultaneously (Figure 1b, arrow ②).

Non-Uniform VMAT Algorithm

The complexity degree of MLC movements related to the VMAT modulation intensity in the different gantry angles, and can be optimized to improve the treatment quality.¹³ Considering that the neighboring segments contribute unequally to the central segment, the affecting factor of the neighboring segment should decrease as the angle increases. We use a Gaussian function to simulate this decreasing effect.

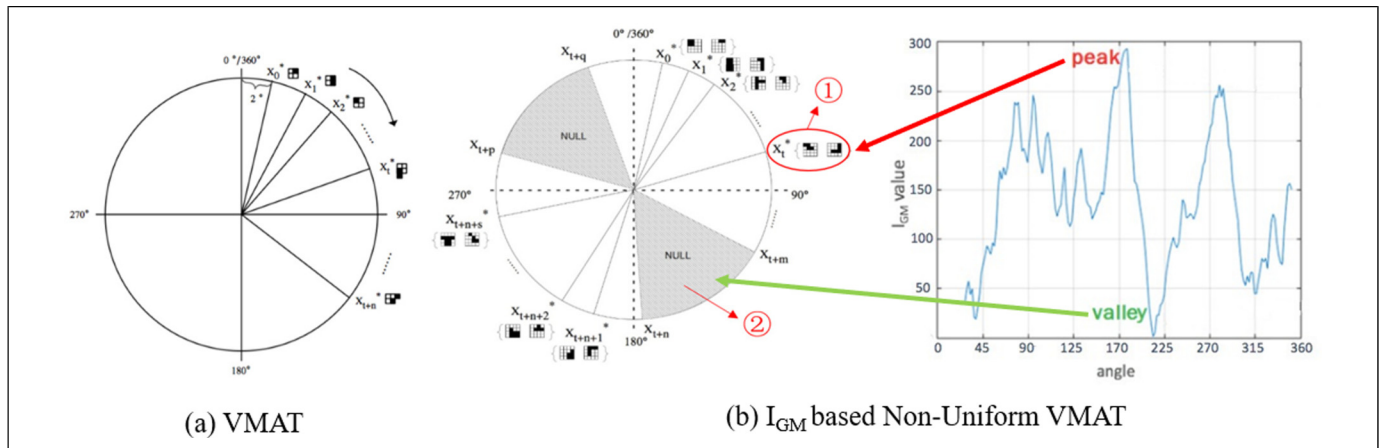


Figure 1. Mathematical model of Homogeneous VMAT (a) and I_{GM} based NU-VMAT (b). (The arc was evenly divided into numerous sub-fields $[x_0, x_1 \dots]$ to obtain the fluence map. Adjacent sub-fields could be combined to reduce the total number of sub-fields [arrow ①] and to ensure the quality of optimization accuracy. After merging, some areas had no radiation distribution, forming “beam-off fields” [arrow ②] to reduce unnecessary radiation); I_{GM} curve which had the complexity degree of MLC movements related to the VMAT modulation intensity in different gantry angles had peak and valley areas (b)).

Abbreviations: NU-VMAT, Non-Uniform Volumetric Modulated Arc Therapy; VMAT, Volumetric Modulated Arc Therapy; MLC, Multi-Leaf Collimator.

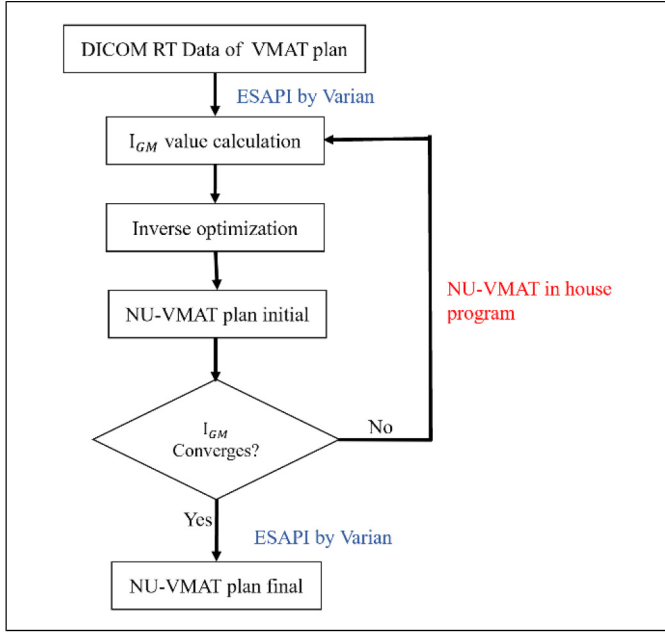


Figure 2. NU-VMAT technology flowchart (The optimization iteration had 2 stages: first, the conventional VMAT plan was optimized in Eclipse® according to dose constraints as usual; then the optimized plan data was exported and the arc range was optimized outside Eclipse by our in-house developed code, optimized arc range was then imported back to Eclipse® to start a new optimization iteration until we got out NU-VMAT plan automatically, which met all clinical requirements and the IGM curve converged obviously. The ESAPI by Varian was the communication interface between Eclipse and our independent program).

Abbreviations: NU-VMAT, Non-Uniform Volumetric Modulated Arc Therapy; VMAT, Volumetric Modulated Arc Therapy; ESAPI, Enterprise Security Application Programming Interface.

A Gantry MLC Movement coefficient Index, I_{GM} , was defined to describe the VMAT modulation intensity

$$I_{GM(n)}(s) = \sum_{K=-K}^K \{g(\delta_a|\mu, \sigma^2) * A_k * [MU(s) - MU(s+k)]\}$$

where $g(\delta_a|\mu, \sigma^2)$ is the Gaussian function with $\mu=0$ which involves the distance influence at different angles. MU is the cumulative monitor units, and A_k is defined as follows:

$$A_k = \sum \rho_i (|x_i^A(s+k-1) - x_i^A(s+k)| + |x_i^B(s+k-1) - x_i^B(s+k)|)$$

where $x_i^A(s+k)$ and $x_i^B(s+k)$ are the i th MLC leaf positions at banks A and B at the $(s+k)$ th station control points, and ρ_i is the thickness of the i th MLC leaf.

Since the I_{GM} value varies as the beam's MU changes, we normalize the I_{GM} value to get a relative percentage (%) of I_{GM} value and this normalized I_{GM} value is not affected by the beam MU. Hence, it is used to be a proper evaluation index to quantitatively describe the beam modulation index at each angle spot (Figure 1). For the evaluation of high and low modulation intensity, high modulation intensity (peak in the curve) is defined as I_{GM} value larger than 150% of the average I_{GM} (Figure 1, left, arrowⓉ), while low modulation intensity (valley in the curve) is defined as the I_{GM} value less than 50% of the average I_{GM} (Figure 2, left, arrowⓂ). High and low modulation intensity areas can be distinguished by comparing I_{GM} value in the gantry range of 30° centers on the peak/valley ($Avg_{\text{peak/valley}}$) and average I_{GM} for all the angles (Avg_{360°).

NU-VMAT Technology Flowchart

All the research data including DICOM images and DICOM RT files of selected patients were retrieved from the clinic database in Eclipse® 15.5 treatment planning system (Varian Medical System). The NU-VMAT program written in Python 3.7 is capable of inputting and outputting DICOM images and DICOM RT files via ESAPI software interface (which was embedded in Eclipse®, licensed by Varian Medical System) automatically. The work flowchart is shown in Figure 2.

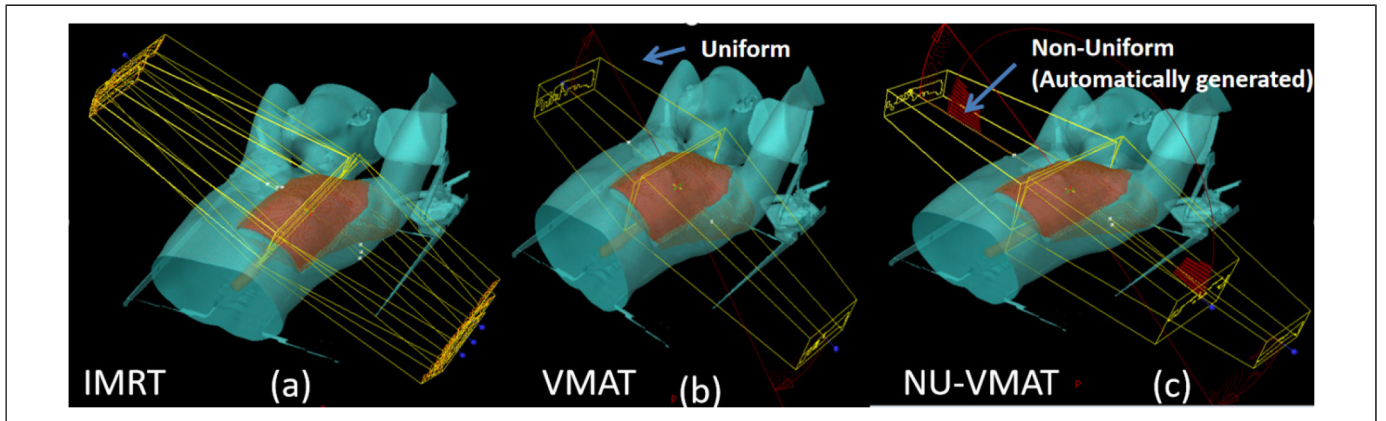
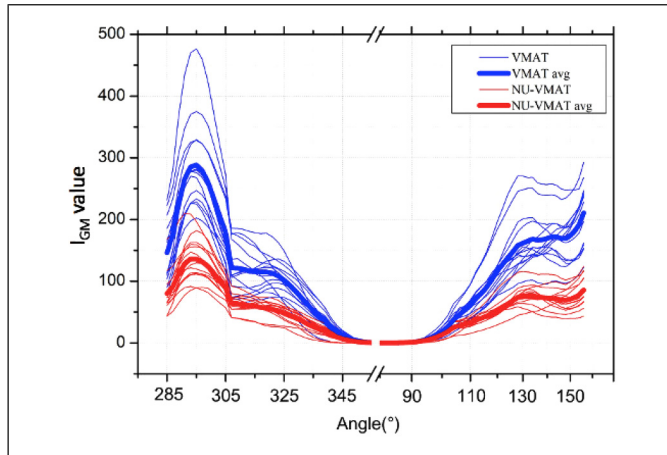


Figure 3. Representative irradiation field distribution from plans designed with indicated technique. (a) IMRT with 6 tangential fields; (b) VMAT with 2 uniform tangential arcs; (c) NU-VMAT with 2 non-uniform tangential arcs.

Abbreviations: IMRT, intensity-modulated radiation therapy; NU-VMAT, Non-Uniform Volumetric Modulated Arc Therapy; VMAT, Volumetric Modulated Arc Therapy.

Table 1. Primary Planning Objectives for the Critical Structures and Target Volumes.

Items	Requirements
PTV	Maximum dose <110% prescribed dose Coverage: V100%prescribed dose \geq 90% PTV
Ipsilateral lung	$V_5 \leq 65\%$, $V_{10} \leq 50\%$, $V_{20} \leq 30\%$, MLD ≤ 12 Gy
Heart	$D_{\text{mean}} \leq 7$ Gy, $V_{25} \leq 25\%$
Skin	Max dose ≤ 8 Gy

**Figure 4.** I_{GM} curve of the VMAT (in blue) and NU-VMAT (in red) for 14 breast cancer cases (the blue and red thick solid line represent the average curve of all VMAT cases and NU-VMAT cases, respectively). Abbreviations: NU-VMAT, Non-Uniform Volumetric Modulated Arc Therapy; VMAT, Volumetric Modulated Arc Therapy.

Patient Data

Fourteen left-sided breast cancer patients treated with BCS and adjuvant whole-breast radiotherapy in the period of November 2019 through June 2020 were randomly selected for this treatment planning study. The average patient age at treatment was 47 (range from 38 to 56). In addition, enrolled patients should meet the following inclusion criteria: (a) *pathological confirmation* of breast cancer; (b) only left-sided breast cancer without contralateral tumor (ie, right-sided cancer); (c) the size of the primary tumor should be < 5 cm; (d) negative axillaries or neck lymph nodes; (e) lack of distant metastasis.

CT Simulation and Contouring

All patients were scanned in a large aperture CT simulator (SOMATOM Definition AS®, Siemens, Germany) in the supine position with upper arm abduction using the immobilization device (Q-fix® breast bracket). The simulation CT images were acquired at a slice thickness of 3 mm covering a range from above the mandible to several centimeters below the inframammary fold, including the entire chest. The attending radiation oncologist with expertise in breast cancer delineated the excision cavity represented by the architectural tissue distortion

and surgical clips. The clinical target volume (CTV) included the glandular tissues of the ipsilateral breast but excluded the pectoralis major or the ribs. The PTV was generated by an extension of 10 mm of CTV but restricted to 5 mm below the skin and anterior to the lung-chest wall interface. The normal structures and OARs, including skin, contralateral breast, thyroid, lungs, and heart were contoured by dosimetry staff and confirmed by the attending radiation oncologist. For skin evaluation, the skin volume was defined as a 3-mm bandwidth from the surface of the breast inwards. The skin dose was defined as the mean maximum dose received by 1% of the skin volume.

3D Treatment Planning Designing

All the treatment plans were designed in Varian Eclipse® system (version 15.5) using an anisotropic analytical dose calculation algorithm (AAA) with a grid of 2.5 mm^3 and the same constraints were used in the inverse optimization. The prescription dose was 50 Gy in 25 fractions with 100% prescription dose covering 90% PTV. Subsequently, treatment plans were simulated in Vitalbeam™ Linear Accelerator, with an energy of 6 MV and a dose rate of 600 MU/min. Sliding window techniques with heterogeneity corrections (the minimum field size $> 4 \text{ cm}^2$) were used.

To protect the OARs, including heart, ipsilateral lung, contralateral lung, and breast, a dynamic sliding window with a fixed gantry angle was used in IMRT technology. Six opposed tangential fields were set with slight adjustment according to anatomical position (Figure 3a).¹⁴ Since these patients have completed their IMRT treatment, the previous IMRT plans were used for comparison directly.

Two tangential arcs were used manually in the VMAT plan according to the tumor position and the normal tissue location (Figure 3b). These 2 tangential arcs should cut fewer lung tissue, with each arc in the range of 30° to 35° .

Based on the previous VMAT plans, NU-VMAT plans were generated automatically through an I_{GM} curve analysis process. In this process, those segments with both lower I_{GM} values and larger cardiac exposure areas in the MLC aperture were removed from the arc intelligently. Since these removed segments had a negligible contribution to the target, the target DVH remained the same while the cardiac DVH improved evidently (Figure 3).

These cases were optimized equally by the same constraints, using conventional IMRT, VMAT, and NU-VMAT technology to analyze the dosimetric differences between these 3 techniques in Eclipse®15.5 treatment planning system.

Dosimetric Evaluation and Treatment Efficiency Parameters

For all treatment plans, dosimetric parameters calculated for the OARs and PTV were listed in Table 1. $D_{1\%}$ was the maximum dose received by 1% of the evaluated OARs volume or PTV selected to avoid point dose influence. $D_{99\%}$ was the minimum dose received by 99% of the evaluated OARs volume or the PTV volume (recommended by the latest

Table 2. The Dosimetric and Efficiency Parameters Comparison Among IMRT, VMAT, and NU-VMAT Plans.

Variables	IMRT (mean ± SD)	VMAT (mean ± SD)	NU-VMAT (mean ± SD)	<i>P</i>		
				IMRT vs VMAT	VMAT vs NU-VMAT	IMRT vs NU-VMAT
<i>Dosimetric evaluation parameters</i>						
PTV						
Volume (cm ³)	694.51 ± 51.98					
D _{1%} (Gy)	52.30 ± 0.80	57.10 ± 0.59	53.96 ± 0.69	.956	.841	.913
D _{99%} (Gy)	46.39 ± 0.70	43.56 ± 0.59	44.19 ± 1.35	.727	.409	.343
D _{mean} (Gy)	50.61 ± 0.76	52.93 ± 0.51	52.09 ± 0.12	.845	.025*	.12
CI	1.22	1.24	1.21	.223	.31	.214
Ipsilateral lung						
Volume (cm ³)	1086.97 ± 67.17					
D _{mean} (Gy)	11.69 ± 0.53	16.85 ± 0.42	14.77 ± 0.39	.633	.629	.397
D _{1%} (Gy)	48.27 ± 0.79	52.63 ± 0.53	50.86 ± 0.33	.949	.175	.506
V ₂₀ (%)	22.51 ± 1.05	32.74 ± 0.99	28.39 ± 1.01	.878	.724	.859
V ₁₀ (%)	33.12 ± 1.49	52.34 ± 1.42	44.23 ± 1.29	.955	.64	.619
V ₅ (%)	42.55 ± 1.62	67.37 ± 1.76	58.20 ± 1.20	.79	.29	.426
D ₅ (Gy)	45.86 ± 1.07	49.58 ± 0.53	48.13 ± 0.39	.507	.327	.263
Heart						
Volume (cm ³)	488.99 ± 25.11					
D _{1%} (Gy)	42.72 ± 2.21	46.02 ± 1.51	41.84 ± 2.14	.064	.154	.747
D _{mean} (Gy)	5.63 ± 0.61	7.94 ± 0.52	5.38 ± 0.46	.531	.982	.475
V ₅ (%)	21.31 ± 1.88	37.24 ± 2.28	25.52 ± 1.90	.401	.32	.812
D ₂₀ (Gy)	5.70 ± 0.67	12.89 ± 1.16	7.69 ± 0.87	.15	.531	.282
D ₃₀ (Gy)	4.35 ± 0.38	7.53 ± 0.81	3.41 ± 0.32	.035*	.023*	.952
Skin						
D _{1%} (Gy)	54.023 ± 0.96	59.10 ± 0.79	56.23 ± 0.30	.029*	.75	.251
<i>Treatment efficiency parameter</i>						
MU	864.4 ± 171.2	245.7 ± 11.1	261.6 ± 41.5	.048*	.129	.020*
Delivery time (min)	3.38 ± 2.9	1.34 ± 0.3	2.42 ± 0.7	.001*	.072	.046*

Abbreviations: IMRT, intensity-modulated radiation therapy; NU-VMAT, Non-Uniform Volumetric Modulated Arc Therapy; VMAT, Volumetric Modulated Arc Therapy; MU, monitor unit; CI, Conformity index; PTV, planning target volume.

*The significant difference existed ($P < .05$). SD: standard deviation.

International Commission on Radiation Units and Measurements Standards.¹⁵ For the ipsilateral breast, the V_5 , V_{10} , and V_{20} described the percentage of breast volumes receiving 5%, 10%, and 20% of the prescribed dose, respectively. The conformity index (CI) is included to reflect the lower isodose line distribution, which was defined as $CI = V_{RI} / V_{PTV}$, where V_{RI} is 100% of the reference isodose volume and the V_{PTV} is the volume of PTV.¹⁶

DVH analysis for the normal structures such as the heart, ipsilateral lung, and skin was performed to assess dosimetric characteristics in all the plans. The constraints and acceptance of normal tissues were listed in Table 1. Most parameters are in accordance with the Radiation Therapy Oncology Group (RTOG) 1304 trial. For treatment efficiency assessment, treatment time (beam-on time plus gantry rotation time) and monitor units were recorded and compared.

Quality Assurance

All plans were validated with standard quality assurance (QA) procedures, including absolute doses and plane dose

measurement verification. The point doses were measured with an ion chamber ($d = 0.6$ cm, TW30013; PTW Dosimetry, Freiburg, Germany) using a solid water phantom. The dose distributions on the 2D plane were assessed using Portal Dosimetry device (Varian Medical System). At least 95% of the pixels should pass the gamma criterion of 3%/3 mm diagnostic test accuracy with a 5% threshold used for NU-VMAT plane dose QA in our institution.¹⁷

Statistical Analysis

The statistical significance of the difference between the groups was assessed using Wilcoxon signed-rank test by SPSS software, release 13.0, and the statistical significance was $P < .05$.

Results

I_{GM} Optimization for VMAT and NU-VMAT

With the iterative optimization using the NU-VMAT model, the $I_{GM-NUVMAT}$ converged significantly in comparison with

I_{GM}^{VMAT} ($P < .05$, Figure 4). The average I_{GM}^{VMAT} curve of all cases ranged from 0% to 297% and $I_{GM}^{NU-VMAT}$ from 50% to 147%. The optimized tangential arcs in NU-VMAT treatment plans distributed in the range of 120° to 140° and 285° to 335°, slightly different from the original VMAT plans (110°-150° and 285°-335°).

PTV Dose Evaluation

The average PTV volume was $694.51 \pm 51.98 \text{ cm}^3$ and the average PTV $D_{1\%}$, D_{mean} , and $D_{99\%}$ from 3 techniques are shown in Table 2 and Figure 5. There was no significant difference among the VMAT, IMRT, and NU-VMAT techniques in terms of PTV parameters, except D_{mean} between the VMAT plan and NU-VMAT plan ($P = .025$). The CI values of NU-VMAT (CI = 1.21) were slightly lower than IMRT (CI = 1.22) and VMAT (CI = 1.24), indicating the favorable performance in conformity and homogeneity of PTV coverage (Table 2, Figures 5 and 6).

OAR Dose Evaluation

The estimated dosimetric parameters in all plans met the criteria specified in the RTOG protocol. Significant differences were seen in the dose received by 30% volume of the heart (D_{30}), with a decrease of 42.28% and 54.79% in NU-VMAT over IMRT and VMAT, respectively. Besides, the NU-VMAT technique resulted in a relatively low D_{mean} in the heart when compared with the VMAT ($P = .982$) and IMRT ($P = .475$) technique. It was evident that the NU-VMAT had better performance in OAR sparing than conventional VMAT and IMRT,

except slight but insignificant dose increase in the left lung in comparison with the IMRT plans (Figures 5 and 6).

Treatment Efficiency

Statistically significant differences were found in the delivery time and machine monitor unit when comparing IMRT with VMAT and NU-VMAT ($P < .05$). MU and the delivery time decreased by 69.8% and 28.4% in NU-VMAT over IMRT ($P < .05$), respectively.

Dose Verification: QA of NU-VMAT

In the NU-VMAT plans, the average absolute dose difference for point dose measurement was $2.4\% \pm 0.19$ (range from 2.2% to 2.7%). For plane dose verification, under the criterion of 3%/3 mm with a 5% threshold and 90% pass rate in the gamma analysis, the average pass rate was $96.5\% \pm 1.11$ (range from 95.3% to 98.1%). And the results indicated that minimal pass rates of DTA > 97% were observed in the IMRT and V-MAT plans, respectively. And the average absolute dose difference for point dose measurement was < 3% in the IMRT and VMAT plans, respectively.

Discussion

In this study, we developed non-uniform VMAT to optimize the treatment of left breast cancer radiotherapy and assessed its effectiveness and feasibility using clinical patient data.

Radiotherapy Technology Optimization and Renovation

IMRT and VMAT are the current mainstay treatment planning techniques in radiotherapy. Many scholars conducted researches related to IMRT and VMAT treatment optimization and successfully verified their reliability.^{13,18-23} Craft et al¹⁸ designed a VMERGE algorithm to make the VMAT planning faster and to explore the tradeoffs between planning objectives and delivery efficiency. Li and Xing¹³ proposed a segmentally boosted VMAT technique in which achieved better OAR sparing and better target coverage. Mullins et al²⁰ tested a non-coplanar “baseball stitch” trajectory which shortened the SAD to optimized VMAT plans. Long et al²¹ improved upon conventional leaf sequencing to incorporate continuous leaf positions explicitly into the treatment planning model. Lyu et al²² developed a novel integrated optimization method for VMAT which decreased the limitation imposed by the square beamlet from the MLC leaf thickness and achieved higher modulation resolution. Papp and Unkelbach²³ also proposed a novel optimization model for VMAT planning that directly optimized leaf trajectory in the treatment plan. To quantitatively analyze the VMAT modulation intensity in this study, the I_{GM} is introduced based on Xing’s modulation index function. In the NU-VMAT model, the relationship between the gantry angle and

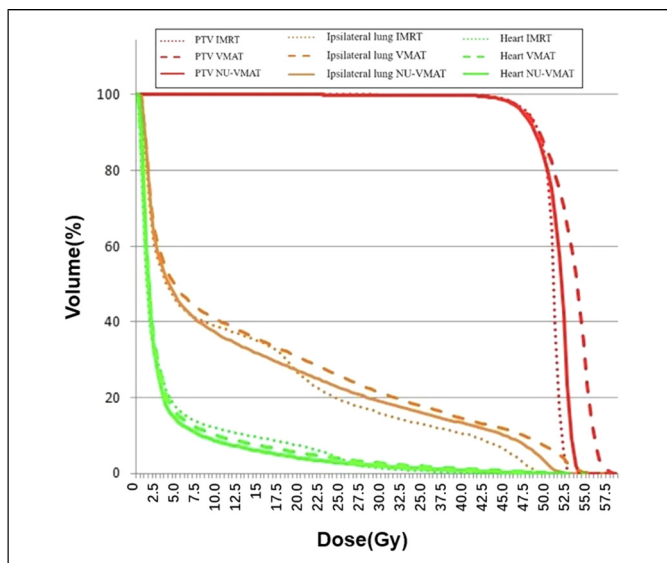


Figure 5. Comparison of the DVH of one case under the 3 techniques: VMAT (dashed thick line), NU-VMAT (solid line), and IMRT (dashed thin line).

Abbreviations: NU-VMAT, Non-Uniform Volumetric Modulated Arc Therapy; VMAT, Volumetric Modulated Arc Therapy; DVH, dose-volume histogram.

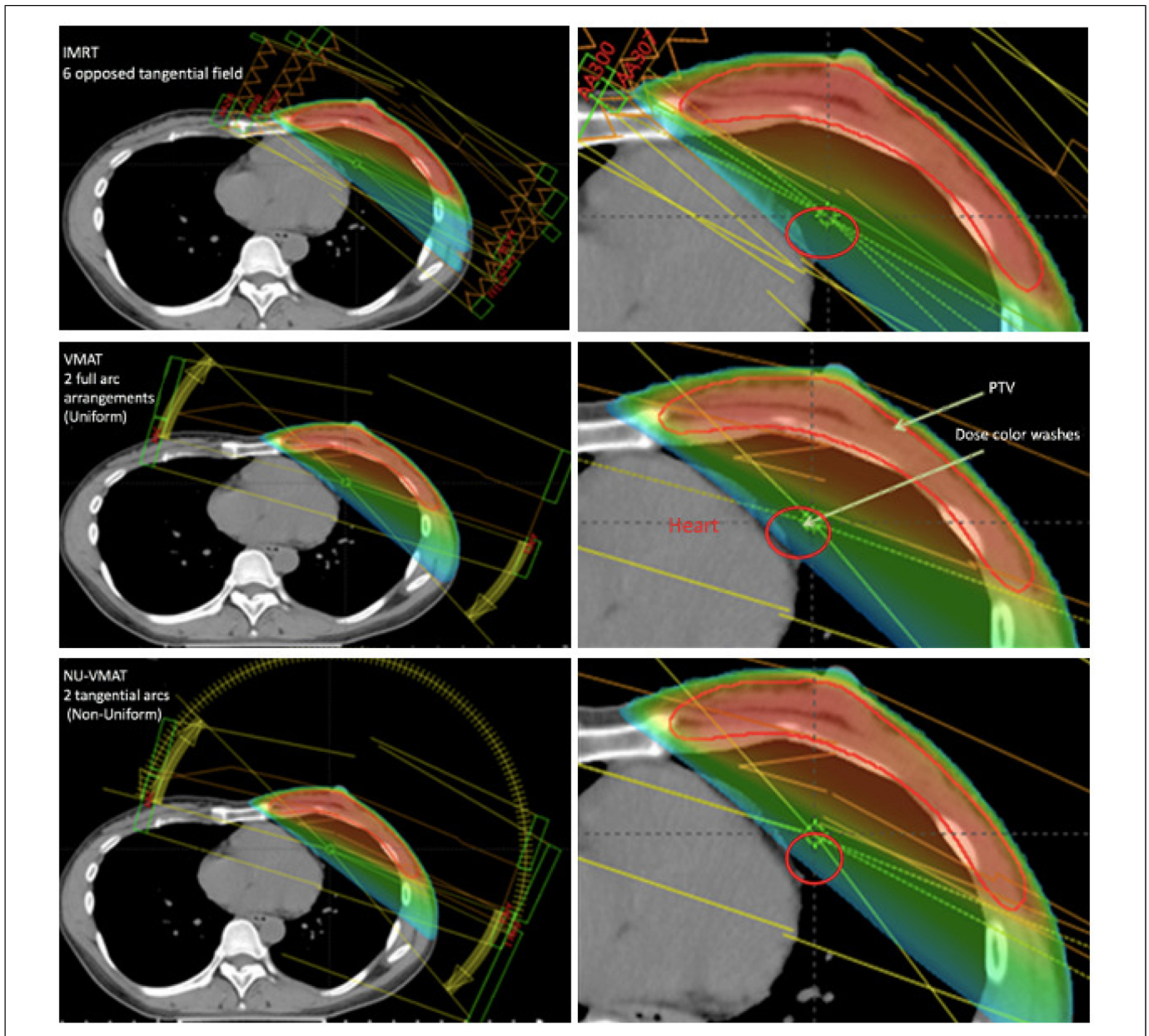


Figure 6. Dose color wash map of 3 techniques: (the red circles represent different dose distributions in the 3 treatment plans).

contribution of neighboring segments to central segments was taken into consideration to better optimize the algorithm.

It is inevitable to radiate the heart during left breast cancer radiotherapy treatment due to the anatomical position of the heart and left breast.²⁴⁻²⁶ Cardiac toxicity was considered to be the most serious radiation-related complication in breast radiotherapy. According to the study from Mege et al, an increment of 1 Gy to the mean heart dose could increase the risk of coronary artery disease by 7.4%.⁵ Karpf et al¹⁰ used tangential-IMRT and tangential-VMAT to optimize the left breast irradiation plans, IMRT decreased the D_{mean} of heart with the reduction of 26.6% compared with VMAT. Wang et al¹¹ reported that IMRT based KBP optimization decreased

heart D_{mean} by 1.3% to 2.2% in comparison with VMAT. Using control points optimization, NU-VMAT achieved better dose control and lower mean dose in the heart (5.38 ± 0.46 Gy) when compared with the VMAT (7.95 ± 0.52 Gy, $P = .982$), resulting in a 32.2% reduction over VMAT and 4.4% reduction over IMRT (5.63 ± 0.61 Gy, $P = .475$).

MU and Delivery Efficiency

NU-VMAT model was designed based on the VMAT technique by eliminating negligible segments of the fields while increasing the weights of significant segments. Hence, the NU-VMAT model keeps the advantages of VMAT while

adding some other benefits including better delivery efficiency and machine output. The reduction in total MUs has the dual benefits of reduced treatment time and less total body scatter dose.¹⁹ In our study, NU-VMAT substantially decreases the machine monitor unit to nearly 69.8% of IMRT. Moreover, the delivery time of NU-VMAT declined by 28.4% comparing to IMRT. Reduced treatment time and improved efficiency certainly favor the control of patients' movement and compliance during radiotherapy.

Conclusion

This study successfully established a new technique (NU-VMAT) for radiotherapy planning which could improve the quality of treatment plan and the efficiency of radiation therapy, and offer better protection for the normal tissue. The preliminary results showed that this NU-VMAT had a dosimetric advantage in cardiac dose control and efficiency advantage in treatment delivery by reducing MU and delivery time in comparison with the conventional VMAT, which warrants further investigation and validation in more patients and multiple cancer centers.

Acknowledgments

The abstract has been accepted as an e-poster presentation at the 2020 AAPM/COMP Annual Meeting; This work was partially supported by the National Natural Science Foundation of China, Grant No.11505029, Natural Science Foundation of China (grant no. 81472794), Shanghai Municipal Commission of Health (grant nos. 2018BR23 and 20184Y0099), and Shanghai Municipal Commission of Science and Technology (grant no. 18441904400).

Ethical Approval

We have re-provided the ethical approval after review, the date is 2020/06/09. Please contact me if you have further questions. Thank you. I appreciate your time and patience in this matter.


Declaration of Conflicting Interests

The authors declared no potential conflicts of interest with respect to the research, authorship, and/or publication of this article.

Funding

The authors received no financial support for the research, authorship and/or publication of this article.

ORCID iD

Jianjian Qiu PhD  <https://orcid.org/0000-0003-0887-7045>

References

- Carr ZA, Land CE, Kleinerman RA, et al. Coronary heart disease after radiotherapy for peptic ulcer disease. *Int J Radiat Oncol Biol Phys.* 2005;61(3):842-850. doi:10.1016/j.ijrobp.2004.07.708
- Vallis KA, Pintilie M, Chong N, et al. Assessment of coronary heart disease morbidity and mortality after radiation therapy for early breast cancer. *J Clin Oncol.* 2002;20(4):1036-1042. doi:10.1200/JCO.2002.20.4.1036
- Clarke M, Collins R, Darby S, et al. Effects of radiotherapy and of differences in the extent of surgery for early breast cancer on local recurrence and 15-year survival: an overview of the randomised trials. *Lancet.* 2005;366(9503):2087-2106. doi:10.1016/S0140-6736(05)67887-7
- Darby S, McGale P, Correa C, et al. Effect of radiotherapy after breast-conserving surgery on 10-year recurrence and 15-year breast cancer death: meta-analysis of individual patient data for 10 801 women in 17 randomised trials. *Lancet.* 2011;378(9804):1707-1716. doi:10.1016/S0140-6736(11)61629-2
- Darby SC, Ewertz M, McGale P, et al. Risk of ischemic heart disease in women after radiotherapy for breast cancer. *N Engl J Med.* 2013;368(11):987-998. doi:10.1056/NEJMoa1209825
- Palumbo I, Mariucci C, Falcinelli L, et al. Hypofractionated whole breast radiotherapy with or without hypofractionated boost in early stage breast cancer patients: a mono-institutional analysis of skin and subcutaneous toxicity. *Breast Cancer.* 2019;26(3):290-304. doi:10.1007/s12282-018-0923-z
- Lancellotta V, Chierchini S, Perrucci E, et al. Skin toxicity after chest wall/breast plus level III-IV lymph nodes treatment with helical tomotherapy. *Cancer Invest.* 2018;36(9-10):504-511. doi:10.1080/07357907.2018.1545854
- Lancellotta V, Iacco M, Perrucci E, et al. Comparing four radiotherapy techniques for treating the chest wall plus levels III-IV draining nodes after breast reconstruction. *Br J Radiol.* 2018;91(1086):20160874. doi:10.1259/bjr.20160874
- Lancellotta V, Iacco M, Perrucci E, et al. Comparison of helical tomotherapy and direct tomotherapy in bilateral whole breast irradiation in a case of bilateral synchronous grade 1 and stage 1 breast cancer. *Am J Case Rep.* 2017;18:1020-1023. Published 2017 Sep 22. doi:10.12659/ajcr.905245
- Karpf D, Sakka M, Metzger M, Grabenbauer GG. Left breast irradiation with tangential intensity modulated radiotherapy (t-IMRT) versus tangential volumetric modulated arc therapy (t-VMAT): trade-offs between secondary cancer induction risk and optimal target coverage. *Radiat Oncol.* 2019;14(1):156. Published 2019 Sep 2. doi:10.1186/s13014-019-1363-4
- Wang J, Hu W, Yang Z, et al. Is it possible for knowledge-based planning to improve intensity modulated radiation therapy plan quality for planners with different planning experiences in left-sided breast cancer patients? *Radiat Oncol.* 2017;12(1):85. Published 2017 May 22. doi:10.1186/s13014-017-0822-z
- Qiu JJ, Chang Z, Wu QJ, Yoo S, Horton J, Yin FF. Impact of volumetric modulated arc therapy technique on treatment with partial breast irradiation. *Int J Radiat Oncol Biol Phys.* 2010;78(1):288-296. doi:10.1016/j.ijrobp.2009.10.036
- Li R, Xing L. An adaptive planning strategy for station parameter optimized radiation therapy (SPORT): segmentally boosted VMAT. *Med Phys.* 2013;40(5):050701. doi:10.1118/1.4802748
- Qiu JJ, Chang Z, Horton JK, Wu QR, Yoo S, Yin FF. Dosimetric comparison of 3D conformal, IMRT, and V-MAT techniques for accelerated partial-breast irradiation (APBI). *Med Dosim.* 2014;39(2):152-158. doi:10.1016/j.meddos.2013.12.001
- Vicini F, Winter K, Straube W, et al. A phase I/II trial to evaluate three-dimensional conformal radiation therapy confined to the

- region of the lumpectomy cavity for stage I/II breast carcinoma: initial report of feasibility and reproducibility of radiation therapy oncology group (RTOG) study 0319. *Int J Radiat Oncol Biol Phys.* 2005;63(5):1531-1537. doi:10.1016/j.ijrobp.2005.06.024
16. Feuvret L, Noël G, Mazeron JJ, Bey P. Conformity index: a review. *Int J Radiat Oncol Biol Phys.* 2006;64(2):333-342. doi:10.1016/j.ijrobp.2005.09.028
17. Nelms BE, Simon JA. A survey on planar IMRT QA analysis. *J Appl Clin Med Phys.* 2007;8(3):76-90. Published 2007 Jul 17. doi:10.1120/jacmp.v8i3.2448
18. Craft D, McQuaid D, Wala J, Chen W, Salari E, Bortfeld T. Multicriteria VMAT optimization. *Med Phys.* 2012;39(2):686-696. doi:10.1118/1.3675601
19. Hernando ML, Marks LB, Bentel GC, et al. Radiation-induced pulmonary toxicity: a dose-volume histogram analysis in 201 patients with lung cancer. *Int J Radiat Oncol Biol Phys.* 2001;51(3):650-659. doi:10.1016/s0360-3016(01)01685-6
20. Mullins J, Renaud MA, Heng V, Ruo R, DeBlois F, Seuntjens J. Trajectory-based VMAT for cranial targets with delivery at shortened SAD. *Med Phys.* 2020;47(7):3103-3112. doi:10.1002/mp.14151
21. Long T, Chen M, Jiang S, Lu W. Continuous leaf optimization for IMRT leaf sequencing. *Med Phys.* 2016;43(10):5403. doi:10.1118/1.4962030
22. Lyu Q, O'Connor D, Ruan D, Yu V, Nguyen D, Sheng K. VMAT Optimization with dynamic collimator rotation. *Med Phys.* 2018;45(6):2399-2410. doi:10.1002/mp.12915
23. Papp D, Unkelbach J. Direct leaf trajectory optimization for volumetric modulated arc therapy planning with sliding window delivery. *Med Phys.* 2014;41(1):011701. doi:10.1118/1.4835435
24. Vicini FA, Kestin L, Chen P, Benitez P, Goldstein NS, Martinez A. Limited-field radiation therapy in the management of early-stage breast cancer. *J Natl Cancer Inst.* 2003;95(16):1205-1210. doi:10.1093/jnci/djg023
25. Moon SH, Shin KH, Kim TH, et al. Dosimetric comparison of four different external beam partial breast irradiation techniques: three-dimensional conformal radiotherapy, intensity-modulated radiotherapy, helical tomotherapy, and proton beam therapy. *Radiother Oncol.* 2009;90(1):66-73. doi:10.1016/j.radonc.2008.09.027
26. Marks LB, Kocak Z, Zhou S, et al. The association between the mean heart dose, mean lung dose, tumor location and RT-associated heart and lung toxicity. *Int J Radiat Oncol.* 2005;63(2):S42. doi:10.1016/j.ijrobp.2005.07.075